

GENETICS

Cx26 heterozygous mutations cause hyperacusis-like hearing oversensitivity and increase susceptibility to noise

Li-Man Liu^{1,2†}, Chun Liang^{1,3†}, Jin Chen^{1†}, Shu Fang^{1†}, Hong-Bo Zhao^{1,2*}

Gap junction gene *GJB2* (Cx26) mutations cause >50% of nonsyndromic hearing loss. Its recessive hetero-mutation carriers, who have no deafness, occupy ~10 to 20% of the general population. Here, we report an unexpected finding that these heterozygote carriers have hearing oversensitivity, and active cochlear amplification increased. Mouse models show that Cx26 hetero-deletion reduced endocochlear potential generation in the cochlear lateral wall and caused outer hair cell electromotor protein prestin compensatively up-regulated to increase active cochlear amplification and hearing sensitivity. The increase of active cochlear amplification also increased sensitivity to noise; exposure to daily-level noise could cause Cx26^{+/-} mice permanent hearing threshold shift, leading to hearing loss. This study demonstrates that Cx26 recessive heterozygous mutations are not “harmless” for hearing as previously considered and can cause hyperacusis-like hearing oversensitivity. The data also indicate that *GJB2* hetero-mutation carriers are vulnerable to noise and should avoid noise exposure in daily life.

INTRODUCTION

Autosomal recessive mutations of a gap junction (GJ) gene Cx26 (*GJB2*) cause DFNB1 (DFN: deafness; B: recessive) deafness and account for >50% of nonsyndromic hearing loss in the clinic (1, 2). The carrier frequency of recessive heterozygous mutations could be up to 20% of the general population (3–7). In the clinic, these recessive heterozygous mutation carriers have no apparent hearing loss and are considered normal in hearing. However, whether these Cx26 heterozygote carriers have other hearing dysfunctions remains unclear.

GJs extensively exist in the inner ear (8), including the epithelial cell GJ (ECGJ) network in the cochlear supporting cells and the connective tissue GJ (CTGJ) network in the cochlear lateral wall (Figs. 1A and 7C). However, there is neither GJ nor connexin expression in the auditory sensory hair cells (9–12). GJs in the cochlea participate in many important functions (8), including cochlear development (13, 14), adenosine triphosphate (ATP) releasing for purinergic signaling (8), endocochlear potential (EP) generation (13, 15), and active cochlear amplification (10, 16, 17). Recently, we found that GJs between the cochlear supporting cells also have medial olivocochlear (MOC) efferent nerve innervation and participate in the regulation of active cochlear amplification (18). In particular, this GJ-mediated regulation plays an important role in the slow, long-term efferent effect (18).

Cx26 and Cx30 (*GJB6*) are two predominant connexin isoforms in the cochlea (9, 12, 19–21). Cx26 mutations can cause both congenital deafness and late-onset hearing loss (22). The congenital deafness mainly results from cochlear developmental disorders (13, 14, 23), whereas the late-onset hearing loss is associated with

the reduction of cochlear active amplification (16, 17, 24). Digenic Cx26 and Cx30 heterozygous mutations also could cause nonsyndromic hearing loss (25–27), which results from EP reduction (15, 28) by impairing GJ function in the cochlear lateral wall (15). However, the hypothesized K⁺ recycling impairment in the cochlea is not a deafness mechanism for Cx26 deficiency-induced hearing loss (29). In this study, we report an unexpected finding that different from Cx26 homozygous mutations or knockout (KO)-induced deafness, both Cx26 heterozygous mutation carriers and Cx26^{+/-} heterozygous KO mice have paradoxically hearing oversensitivity, and active cochlear amplification increased, which leads to hyperacusis and vulnerability to noise.

RESULTS

Increase of hearing sensitivity in Cx26^{+/-} hetero-deletion mice

Figure 1 shows that hearing sensitivity increased in Pax2-Cx26^{+/-} hetero-deletion mice. Immunofluorescent staining for Cx26 showed that there was no Cx26 labeling visible in Cx26^{-/-} homozygous deletion or conditional KO (cKO) mice (Fig. 1D). However, the Cx26 labeling was visible in Cx26^{+/-} hetero-deletion mice (Fig. 1C) but weaker than that in wild-type (WT) mice (Fig. 1B). In comparison with WT mice, intensities of Cx26 labeling in the organ of Corti (OC) and cochlear lateral wall in Cx26^{+/-} mice were significantly reduced to 41.7 ± 7.7% ($P < 0.001$, two-tailed t test) and 60.7 ± 9.0% ($P = 0.03$, two-tailed t test), respectively (Fig. 1E). However, Cx30 expression in Cx26^{+/-} mice had no significant change (fig. S1). In comparison with those in WT mice, the expression of Cx30 in the OC and lateral wall in Cx26^{+/-} mice was 80.0 ± 11.4% ($P = 0.22$, two-tailed t test) and 94.0 ± 12.6% ($P = 0.71$, two-tailed t test), respectively (fig. S1B).

Different from deafness in Pax2-Cx26^{-/-} cKO mice (pink lines and symbols in Fig. 1, F and G), hearing sensitivity in Pax2-Cx26^{+/-} mice was enhanced (blue lines and symbols in Fig. 1, F to M). In comparison with WT mice (Fig. 1G), the auditory brainstem

Copyright © 2023 The Authors, some rights reserved; exclusive licensee American Association for the Advancement of Science. No claim to original U.S. Government Works. Distributed under a Creative Commons Attribution NonCommercial License 4.0 (CC BY-NC).

¹Department of Otolaryngology, University of Kentucky Medical Center, 800 Rose Street, Lexington, KY 40536, USA. ²Department of Surgery-Otolaryngology, Yale University Medical School, 310 Cedar Street, New Haven, CT 06510, USA. ³Hearing Function Testing Center, Shenzhen Maternity and Child Healthcare Hospital, 3012 Fuqiang Road, Shenzhen 518017, China.

†These authors contributed equally to this work.

*Corresponding author. Email: hong-bo.zhao@yale.edu

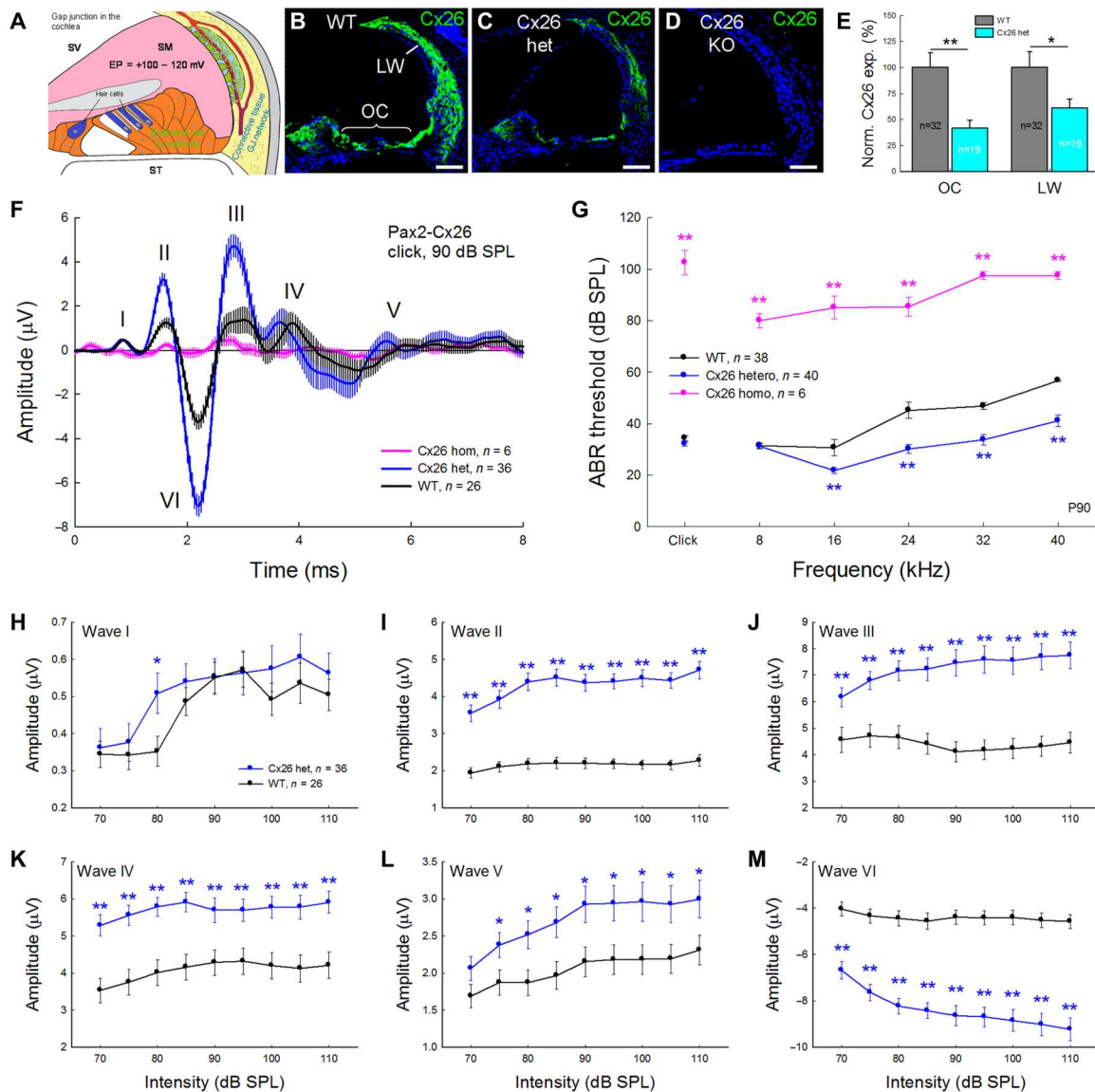


Fig. 1. Increase of hearing sensitivity in Pax2-Cx26^{+/-} hetero-deletion mice. (A) Diagram of GJ network in the cochlea. Hair cells have neither GJ nor connexin expression. SV, scala vestibuli; SM, scala media; ST, scala tympani. (B to D) Immunofluorescent staining for Cx26 (green) in the cochlea. Cx26 has labeling in Cx26^{+/-} mice but the intensity of labeling is weaker than that in WT mice (C). No labeling is visible in Cx26^{-/-} cKO mice (D). OC, the organ of Corti; LW, lateral wall; WT, wild type; KO, knockout. Scale bars, 50 µm. (E) Quantitative analysis of Cx26 labeling at the OC and LW in Pax2-Cx26^{+/-} mice. The intensity of labeling was normalized to the average value in WT mice. The expression of Cx26 in Cx26^{+/-} mice was reduced by ~50%. (F) Averaged ABR traces recorded from WT, Cx26^{+/-}, and Cx26^{-/-} mice. The ABR traces were evoked by 90 dB of sound pressure level (SPL) click stimulations and averaged. Bars represent SEM. Mice were 90 days old. (G) ABR thresholds in Cx26^{+/-} mice were significantly reduced in comparison with those in WT mice. Pink line and symbols represent ABR thresholds recorded from Pax2-Cx26^{-/-} cKO mice, which appeared as severe hearing loss. (H to M) Quantitative measurement of ABR peaks in Pax2-Cx26^{+/-} mice. ABRs were evoked by click stimuli. The amplitudes of waves II to VI in Cx26^{+/-} mice were significantly increased in comparison with WT mice. **P* < 0.05 and ***P* < 0.01, two-tailed *t* test.

response (ABR) thresholds in Cx26^{+/-} mice were significantly reduced by 10 to 20 dB of sound pressure level (SPL) (*P* > 0.01, two-tailed *t* test). The super-threshold ABR recorded from Cx26^{+/-} mice also appeared large responses (Fig. 1F). Quantitative analyses (Fig. 1, H to M) showed that amplitudes of ABR waves II to VI in Cx26^{+/-} mice were significantly larger than WT mice (*P* < 0.05 or *P* < 0.01, two-tailed *t* test) in the tested intensity range (70 to 110 dB SPL).

The similar increase in hearing sensitivity was also found in Foxg1-Cx26^{+/-} hetero-deletion mice (Fig. 2). As observed in Pax2-Cx26^{+/-} hetero-deletion mice (Fig. 1), the super-threshold ABR in Foxg1-Cx26^{+/-} hetero-deletion mice was large (Fig. 2B), and the ABR thresholds were significantly lower at a high-frequency range in comparison with those at WT mice (*P* < 0.01, two-tailed *t* test) as well (Fig. 2C). Quantitative analyses showed that amplitudes of ABR waves II, III, and VI were significantly increased at high intensities (*P* < 0.01 or *P* < 0.05, two-tailed *t* test) (Fig. 2, E, F, and I).

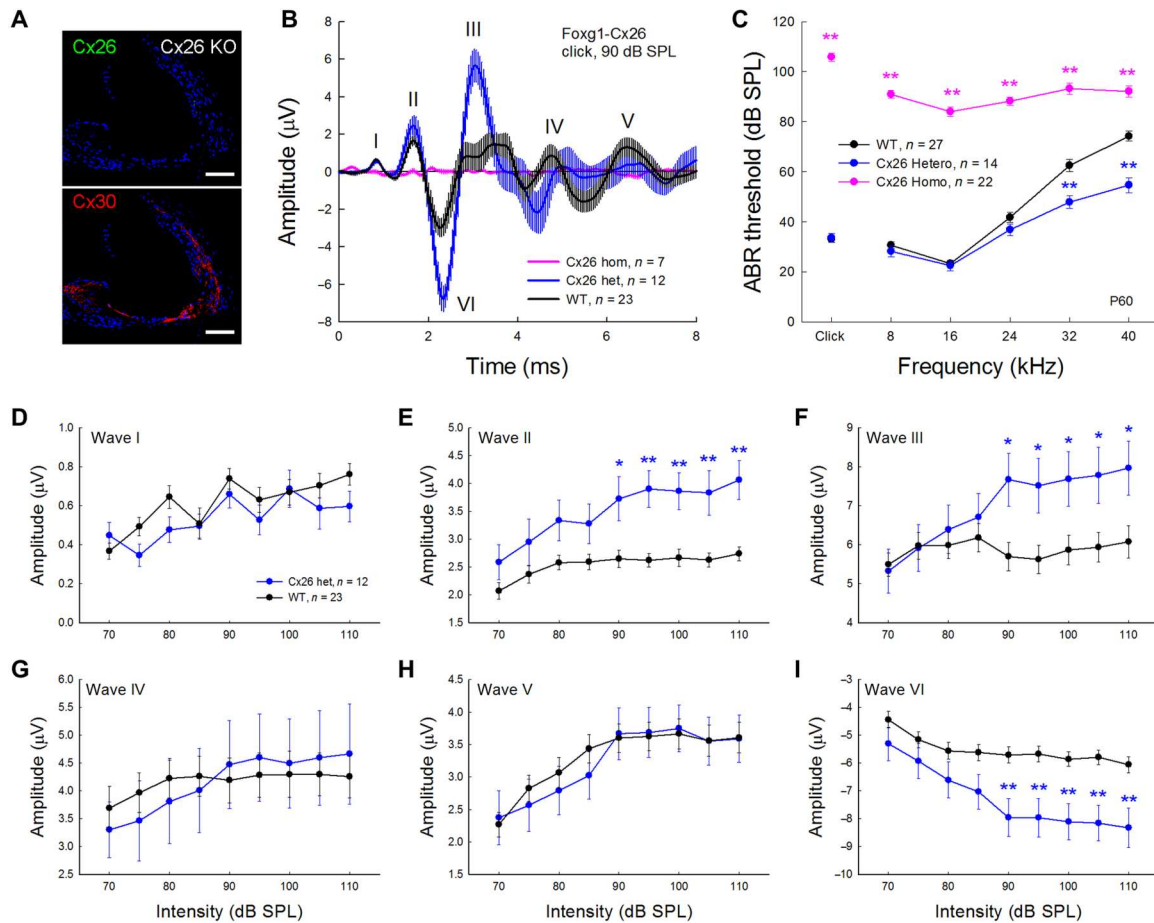


Fig. 2. Increase of hearing sensitivity in Foxg1-Cx26^{+/-} hetero-deletion mice. (A) Cx26 deletion in the cochlea in Foxg1-Cx26^{-/-} cKO mice. Immunofluorescence staining shows negative staining for Cx26 in the Foxg1-Cx26^{-/-} mouse cochlea. Cx30 staining in the cochlea of Cx26^{-/-} mice appears normal. Scale bars, 50 μ m. (B) Averaged traces of ABR recorded from WT, Foxg1-Cx26^{+/-}, and Foxg1-Cx26^{-/-} mice. The traces were evoked by 90 dB SPL of click stimuli and averaged from different mice. Bars represent SEM. Mice were 60 days old. ABR waves in Foxg1-Cx26^{+/-} mice are larger than those in WT mice. The pink line near the base line represents the evoked ABR trace in Foxg1-Cx26^{-/-} cKO mice. (C) ABR thresholds in Foxg1-Cx26^{+/-} mice were significantly reduced in comparison with those in WT mice. WT littermates served as control. Pink lines and symbols represent ABR thresholds recorded from Foxg1-Cx26^{-/-} cKO mice, which appeared as severe hearing loss or deafness. ** $P < 0.01$, two-tailed t test versus WT mice. (D to I) Quantitative measurement of ABR waves in Foxg1-Cx26^{+/-} mice. ABRs were evoked by click stimuli, and the peaks of waves I to VI were measured and averaged. The amplitudes of waves II, III, and VI at high intensities in Cx26^{+/-} mice were significantly increased in comparison with those in WT mice. * $P < 0.05$ and ** $P < 0.01$, two-tailed t test.

For Foxg1-Cx26^{-/-} cKO mice, Cx26 was also absent in the whole cochlea (Fig. 2A), and the ABR thresholds were larger than 80 dB SPL (pink line and symbols in Fig. 2C), showing hearing loss.

Increase of the auditory receptor current in Cx26^{+/-} mice

Cochlear microphonic (CM) is the auditory receptor current/potential. CM in both Pax2-Cx26^{+/-} and Foxg1-Cx26^{+/-} hetero-deletion mice was significantly increased in comparison with that in WT mice (Fig. 3). The CM was increased as intensity was increased (Fig. 3, B and E). At 90 dB SPL, the recorded CMs in Pax2-Cx26^{+/-} and WT mice were $35.8 \pm 3.10 \mu$ V ($n = 36$) and $12.3 \pm 1.07 \mu$ V ($n = 38$), respectively (Fig. 3, B and C). In Foxg1-Cx26^{+/-} mice (Fig. 3, D to F), the recorded CM at 90 dB SPL was $41.8 \pm 6.13 \mu$ V ($n = 12$) and was also significantly increased in comparison with that ($22.0 \pm 3.02 \mu$ V, $n = 22$) in WT mice [$P < 0.01$, one-way analysis of variance (ANOVA) with Bonferroni correction] (Fig. 3F). However, CM in both Pax2-Cx26^{-/-} and Foxg1-Cx26^{-/-}

cKO mice appeared very small near the recording noise level (Fig. 3, A and D) and was $4.58 \pm 1.07 \mu$ V ($n = 8$) and $7.05 \pm 0.741 \mu$ V ($n = 22$), respectively, at 90 dB SPL of stimulated sound intensity (Fig. 3, C and F). In comparison with WT mice, CMs in both Cx26^{-/-} cKO mice were significantly reduced ($P < 0.01$, one-way ANOVA with a Bonferroni correction), consistent with deafness found in both Pax2-Cx26^{-/-} and Foxg1-Cx26^{-/-} cKO mice (Figs. 1G and 2C).

Increase of distortion product otoacoustic emission in Cx26^{+/-} mice

Distortion product otoacoustic emission (DPOAE), which reflects the active cochlear amplification, in Cx26^{+/-} mice was increased (Figs. 4 and 5). DPOAEs in both Pax2-Cx26^{+/-} and Foxg1-Cx26^{+/-} hetero-deletion mice were significantly increased by ~ 10 dB SPL in comparison with that in WT mice ($P < 0.05$ or $P < 0.01$, one-way ANOVA with a Bonferroni correction) (Figs. 4C and 5C). In input/

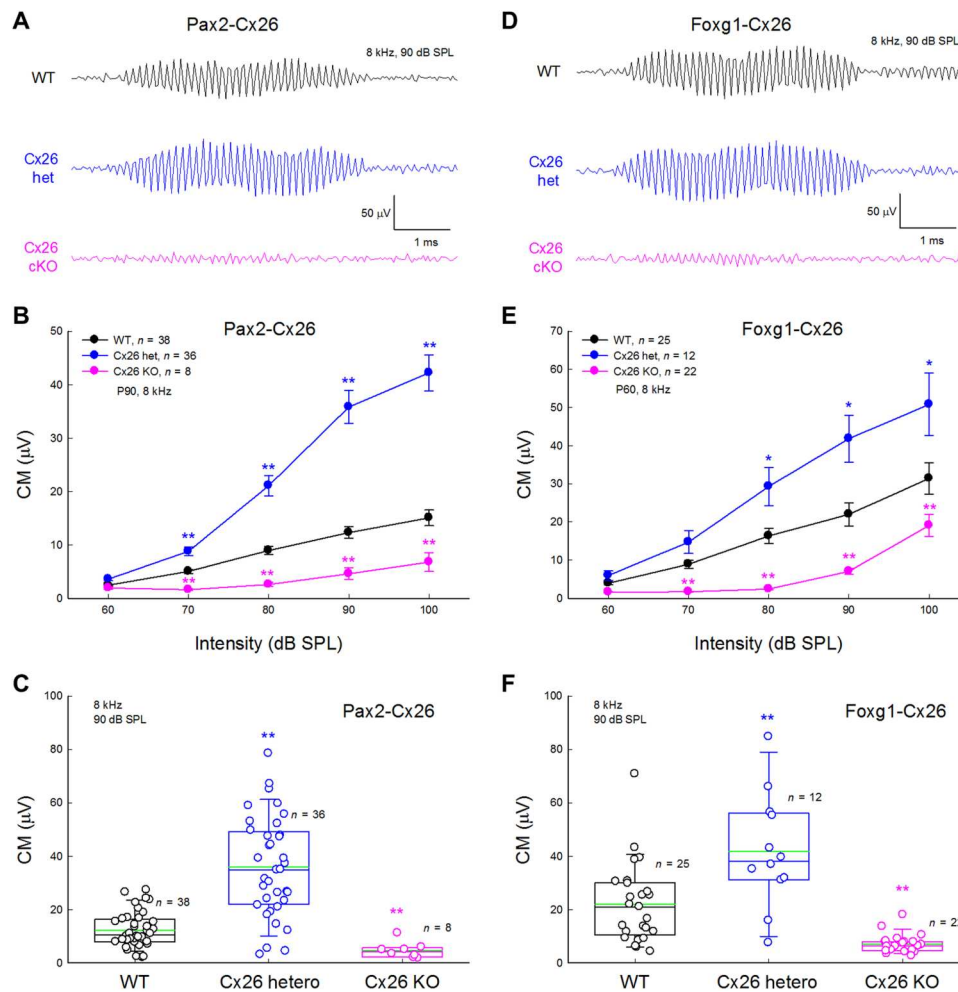


Fig. 3. Increase of CM in Pax2-Cx26^{+/-} mice and Foxg1-Cx26^{+/-} mice. (A) CM traces recorded from WT, Pax2-Cx26^{+/-}, and Pax2-Cx26^{-/-} mice. CM was evoked by 90 dB SPL, 8 kHz of tone bursts. (B) CM in Pax2-Cx26^{+/-} mice was significantly increased in comparison with that in WT mice, whereas CM in Pax2-Cx26^{-/-} cKO mice was significantly reduced. Mice were 3 months old. ****P** < 0.01, two-tailed *t* test versus WT. (C) CM in WT, Pax2-Cx26^{+/-}, and Pax2-Cx26^{-/-} mice at stimulation of 90 dB SPL, 8 kHz of tone bursts. Green lines in the boxes represent the mean levels. In comparison with WT mice, CMs in Pax2-Cx26^{+/-} were significantly increased and CMs in Pax2-Cx26^{-/-} mice were significantly reduced. ****P** < 0.01, one-way ANOVA with a Bonferroni correction. (D to F) CM recorded from WT, Foxg1-Cx26^{+/-}, and Foxg1-Cx26^{-/-} mice by 90 dB SPL, 8 kHz of tone bursts. Mice were 2 months old. In comparison with that in WT mice, CM in Foxg1-Cx26^{+/-} mice was significantly increased while CM in Foxg1-Cx26^{-/-} cKO mice was significantly decreased. ***P** < 0.05 and ****P** < 0.01, two-tailed *t* test versus WT in (E) and one-way ANOVA with a Bonferroni correction in (F).

output (I/O) plots (Figs. 4C and 5C), the increase was visible in most intensity range. The DPOAE gain (i.e., $2f_1-f_2$ re: f_1) in Cx26^{+/-} mice (Figs. 4D and 5D) also increased about 10 dB in comparison with that in WT mice (P < 0.05 or 0.01, one-way ANOVA with a Bonferroni correction). However, there was no DPOAE visible in both Pax2-Cx26^{-/-} and Foxg1-Cx26^{-/-} cKO mice (Figs. 4, B and C, and 5, B and C).

Outer hair cell (OHC) electromotility is a major contributor for active cochlear amplification in mammals. We further examined expression of OHC motor protein prestin in Cx26^{+/-} mice (Fig. 4, E and F). In comparison with WT mice, prestin expressions in the apical, middle, and basal cochlear turn in Cx26^{+/-} mice significantly increased to 149.7 ± 10.2 , 138.9 ± 9.49 , and $127.4 \pm 7.23\%$ (P < 0.05 or P < 0.01, two-tailed *t* test), respectively (Fig. 4F).

EP reduction in Cx26^{+/-} mice

EP is a driving force and is required for hair cells' generating auditory receptor current/potential. We found that EP in Cx26^{+/-} mice was significantly reduced. EP in WT, Cx26^{+/-}, and Cx26^{-/-} mice was 98.2 ± 3.25 mV ($n = 8$), 51.5 ± 3.80 mV ($n = 13$), and 31.3 ± 6.58 mV ($n = 14$), respectively (Fig. 6B). In comparison with WT mice, EPs in Cx26^{+/-} and Cx26^{-/-} mice were significantly reduced by ~50 and ~70%, respectively (P < 0.001, one-way ANOVA with a Bonferroni correction). There was also significant difference between Cx26^{+/-} and Cx26^{-/-} mice ($P = 0.023$, one-way ANOVA with a Bonferroni correction).

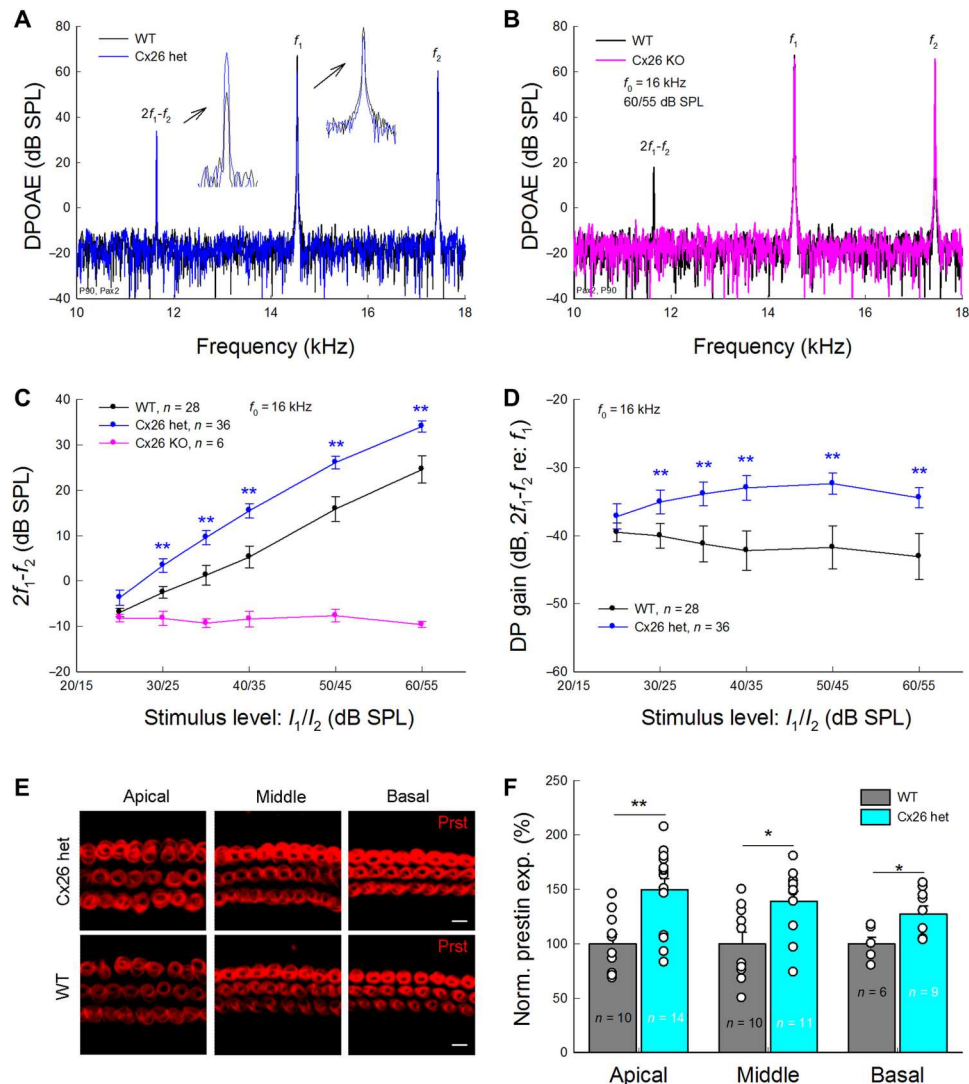


Fig. 4. Increase of DPOAE in Pax2-Cx26^{+/-} mice. (A and B) Spectra of acoustic emission recorded from WT, Cx26^{+/-}, and Cx26^{-/-} mice. Mice were 3 months old. DPOAEs were evoked by two-tone stimulation. $f_0 = 16$ kHz, $I_1/I_2 = 60/55$ dB SPL. Insets: Large-scale plots of $2f_1-f_2$ and f_1 peaks. The peak of DPOAE ($2f_1-f_2$) in Cx26^{+/-} mice was increased, but f_1 and f_2 peaks remained the same as those in WT mice. A pink trace in (B) represents spectrum in Cx26^{-/-} cKO mice. No DPOAE peak is visible. (C) Increase of DPOAE in Cx26^{+/-} mice in the I/O plot. In comparison with WT mice, I/O function of DPOAE in Cx26^{+/-} was shifted up to ~10 dB SPL. However, no DPOAE is recordable in Cx26^{-/-} mice. (D) Gain in distortion product (DP) ($2f_1-f_2$ re: f_1) in Cx26^{+/-} and WT mice. DP gain in Cx26^{+/-} mice was significantly increased by 5 to 10 dB in comparison with WT mice. (E) Increase of prestin expression at outer hair cells (OHCs) in Cx26^{+/-} mice. Immunofluorescent staining for prestin at the cochlear apical, middle, and basal turn in Cx26^{+/-} mice appears more intensive than WT mice. (F) Quantitative measurement of prestin labeling in Cx26^{+/-} and WT mice. The intensity of prestin labeling at the apical, middle, and basal turn in Cx26^{+/-} mice was separately normalized to the average value at the corresponding turn in WT mice. Prestin expressions at all cochlear turns in Cx26^{+/-} mice were significantly increased in comparison with those in WT mice. * $P < 0.05$ and ** $P < 0.01$, two-tailed t test.

Neither EP reduction nor hearing sensitivity enhancement in mice with targeted hetero-deletion of Cx26 in the cochlear supporting cells

EP is generated in the cochlear lateral wall, where the CTGJ network locates at (Figs. 1A and 7C). We further selectively deleted Cx26 expression in the cochlear Deiters cells (DCs) and outer pillar cells in the ECGJ network, i.e., retained Cx26 expression in the CTGJ in the cochlear lateral wall (Fig. 7, A to C) using the Prox1-Cre mouse line as we previously reported (16, 17). Figure 7A shows that Cx26 expression in the cochlear lateral wall in Prox1-Cx26 cKO mice remained normal. EP retained normal as well in Prox1-Cx26^{+/-}

mice (Fig. 7D) and had no significant reduction as observed in Pax2-Cx26^{+/-} mice (Fig. 6). ABR thresholds in Prox1-Cx26^{+/-} mice were also significantly increased, i.e., hearing loss (Fig. 7E), rather than the observed ABR threshold reduction (i.e., hearing sensitivity increased) in both Pax2-Cx26^{+/-} and Foxg1-Cx26^{+/-} mice (Figs. 1G and 2C), which had significant EP reduction (Fig. 6). DPOAE in Prox1-Cx26^{+/-} mice were also significantly reduced (Fig. 7F) rather than increased in Pax2-Cx26^{+/-} and Foxg1-Cx26^{+/-} mice (Figs. 4 and 5).

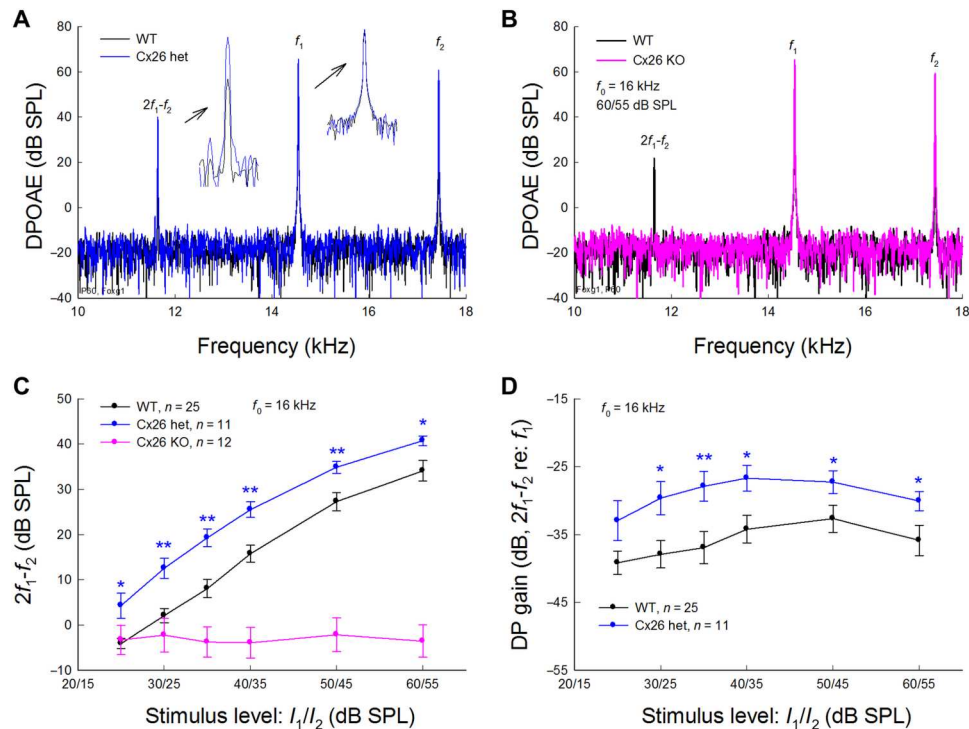


Fig. 5. Increase of DPOAE in Foxg1-Cx26^{+/-} mice. Mice were 2 months old. (A and B) Spectra of acoustic emission recorded from WT, Foxg1-Cx26^{+/-}, and Foxg1-Cx26^{-/-} mice. DPOAEs were evoked by two-tone stimulation. $f_0 = 16$ kHz, $I_1/I_2 = 60/55$ dB SPL. Insets: Large-scale plots of $2f_1-f_2$ and f_1 peaks. The peak of $2f_1-f_2$ in Foxg1-Cx26^{+/-} mice was increased, while f_1 and f_2 peaks remained the same as those in WT mice. A pink trace in (B) represents no DPOAE peak visible in Foxg1-Cx26^{-/-} mice. (C) DPOAE in Foxg1-Cx26^{+/-} mice is increased in comparison with WT mice. I/O function of DPOAE in Foxg1-Cx26^{+/-} was shifted up to ~10 dB SPL. No DPOAE is visible in Foxg1-Cx26^{-/-} mice. (D) DP gain ($2f_1-f_2$ re: f_1) in Foxg1-Cx26^{+/-} mice. In comparison with WT mice, DP gain in Foxg1-Cx26^{+/-} mice was significantly increased by 5 to 10 dB. * $P < 0.05$ and ** $P < 0.01$, two-tailed t test.

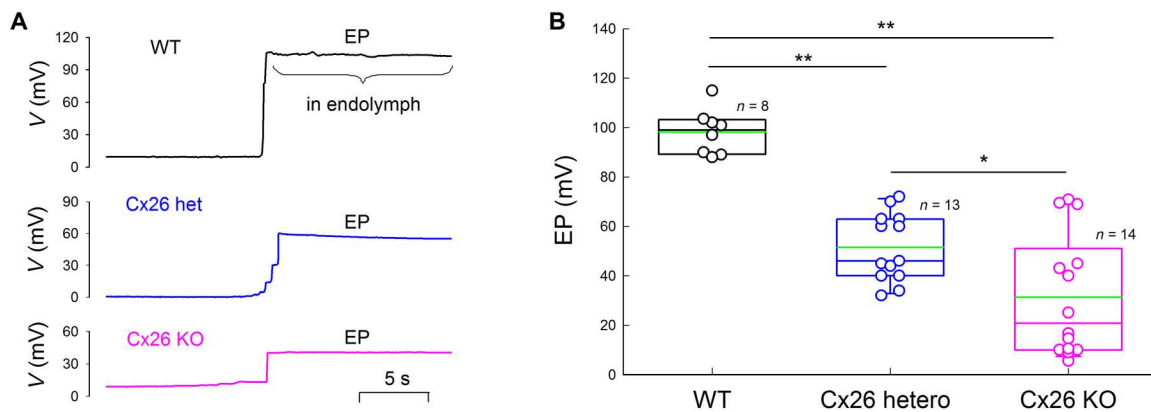


Fig. 6. Reduction of EP in Pax2-Cx26^{+/-} hetero-deletion mice. (A) EP recording traces from WT, Cx26^{+/-}, and Cx26^{-/-} mice. When the recording pipette entered into the endolymph, the potential (i.e., EP) was recordable. (B) EPs in Cx26^{+/-} and Cx26^{-/-} mice were significantly reduced in comparison with that in WT mice. Green lines in boxes represent the mean levels. * $P < 0.05$ and ** $P < 0.01$, one-way ANOVA with a Bonferroni correction.

Increase of susceptibility to noise in Cx26^{+/-} mice

Increase of active cochlear amplification could increase susceptibility to noise (Fig. 8). After exposure to ~96 dB of white noise for 2 hours, one time, ABR thresholds in both Cx26^{+/-} heterozygous mice and WT mice had substantial increase (Fig. 8, A and B). However, ABR thresholds in Cx26^{+/-} mice at a high-frequency range (40 kHz) were higher than those in WT mice (Fig. 8, B and C). At postexposure day 1 (P1), the shift of ABR thresholds at 40

kHz in Cx26^{+/-} and WT mice was 24.4 ± 1.42 dB SPL ($n = 16$) and 12.1 ± 2.55 dB SPL ($n = 14$), respectively. The shift in ABR threshold in Cx26^{+/-} mice was double of that in WT mice (Fig. 8, B and C). There was significant difference between them ($P = 4.2 \times 10^{-4}$, two-tailed t test). The postexposure recovery in Cx26^{+/-} mice also appeared slow and uncompleted (Fig. 8, A and B). At the middle-frequency range (16 kHz), the ABR threshold in WT mice at P28 completely recovered to pre-noise exposure level (Fig. 8A).

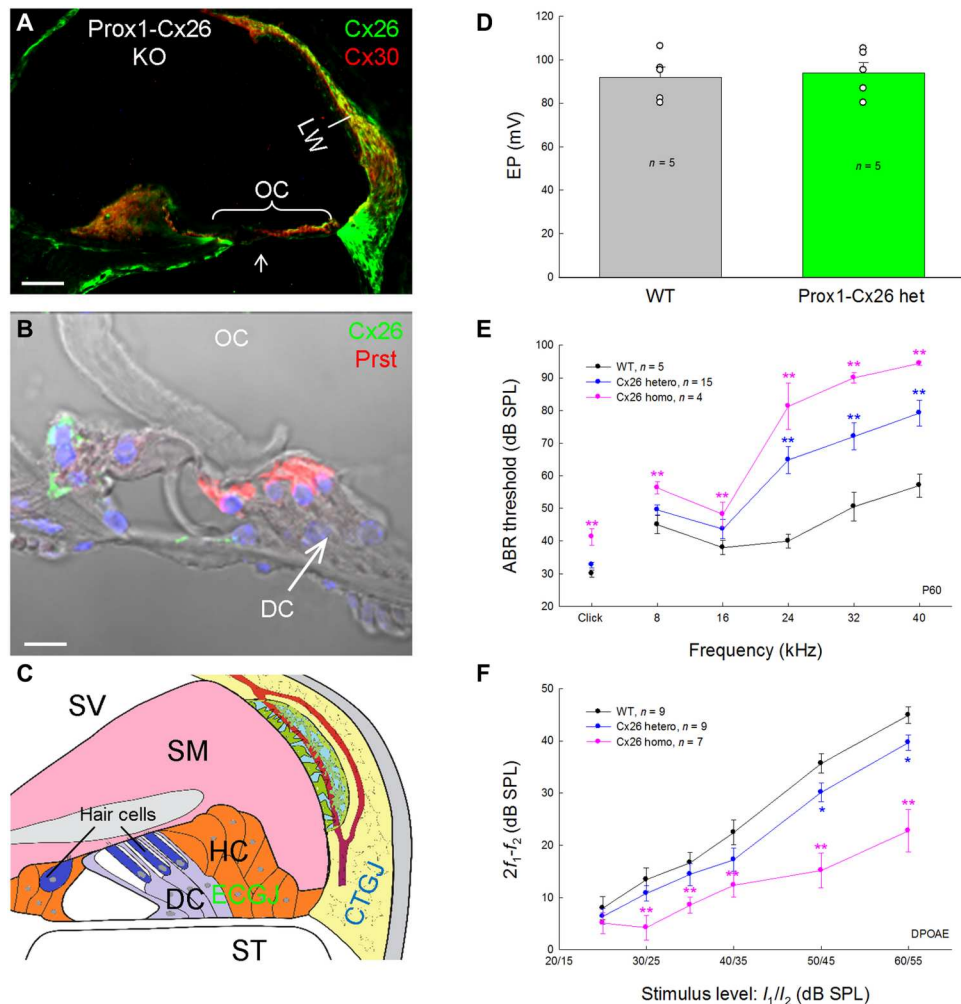


Fig. 7. Decrease rather than increase in hearing sensitivity and active cochlear amplification in Prox1-Cx26^{+/-} hetero-deletion mice. (A) Prox1-Cx26^{-/-} cKO mice have deletion of Cx26 at the cochlear supporting DCs and outer pillar cells but not at the cochlear lateral wall. Scale bar, 50 μ m. (B) A high-magnification image of the OC. An arrow indicates no Cx26 expression at DCs. Red labeling represents immunofluorescent staining for prestin (Prst). Scale bar, 20 μ m. (C) Diagram of deletion of Cx26 in the DCs and outer pillar cells in Prox1-Cx26 cKO mice. Partial Cx26 expression in the ECG network in the cochlear sensory epithelium is deleted in the Prox1-Cx26 cKO mice, while Cx26 expression in the CTGJ network in the cochlear lateral wall remains normal. HC, Hensen cell. (D) EP in Prox1-Cx26^{+/-} mice appears normal. (E) ABR thresholds in Prox1-Cx26^{+/-} mice as Prox1-Cx26^{-/-} cKO mice are significantly increased rather than decreased in comparison with those in WT mice. (F) I/O function of DPOAE in WT, Prox1-Cx26^{+/-}, and Prox1-Cx26^{-/-} mice. Similar to Prox1-Cx26^{-/-} cKO mice, DPOAEs in Prox1-Cx26^{+/-} mice are significantly decreased rather than increased in comparison with those in WT mice. * $P < 0.05$ and ** $P < 0.01$, two-tailed t test.

However, Cx26^{+/-} mice at P28 still had about 11.3 ± 1.02 dB SPL ($n = 16$) of threshold shift (Fig. 8A). There was a significant difference in comparison with the preexposure level ($P < 0.01$, two-tailed t test). The recovery at a high-frequency range in Cx26^{+/-} mice also appeared slow and small (Fig. 8B). At P28, Cx26^{-/-} mice still had 17.1 ± 1.88 ($n = 16$) threshold shift (Fig. 8B). Moreover, in comparison with control Cx26^{+/-} mice without noise exposure, the ABR threshold in noise-exposed Cx26^{+/-} mice at P90 still had 5 to 10 dB of threshold shift ($P < 0.01$, two-tailed t test) (Fig. 8D).

DPOAE in Cx26^{+/-} mice after noise exposure was also significantly reduced (Fig. 9). At P90, DPOAE in noise-exposed Cx26^{+/-} mice was significantly reduced by ~ 10 dB in comparison with control Cx26^{+/-} mice without noise exposure ($P < 0.01$, two-tailed t test) (Fig. 9), consistent with increased ABR threshold in noise-exposed Cx26^{+/-} mice (Fig. 8D).

Increase of hearing sensitivity and active cochlear amplification in Cx26 heterozygous mutation carriers

We further investigated hearing functional changes in human *GJB2* heterozygous mutation carriers. To limit the effects of environmental factors, we recruited children in this study. We recruited 15 *GJB2* single-point heterozygous mutation carriers (eight females and seven males; median age: 117 days) from daily visiting in the clinics, including 13 of *GJB2* c.109G > A (p.V37I) heterozygote carriers (Fig. 10A) and 2 of *GJB2* c.235delC heterozygote carriers (table S1). All of these *GJB2* heterozygote carriers passed the newborn hearing screening tests after birth. The control group had 15 normally delivered, typical development, age-matched children (seven females and eight males; median age: 101 days) (table S1). As observed in Cx26^{+/-} mice, *GJB2* heterozygote carriers also demonstrated both active cochlear amplification and hearing sensitivity

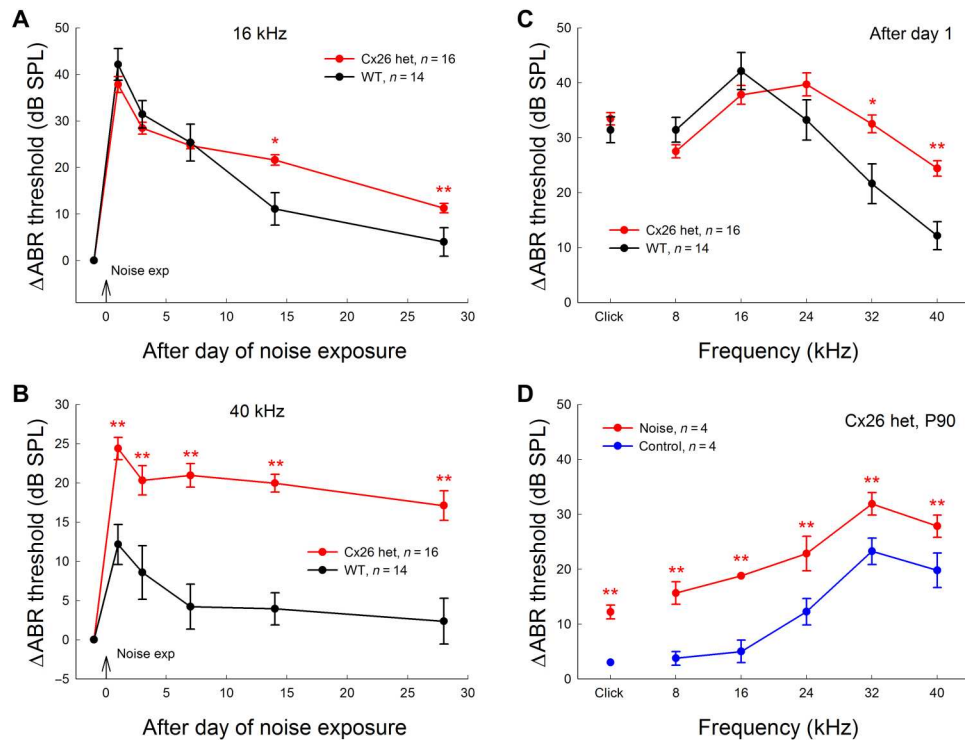


Fig. 8. Increase of susceptibility to noise in Cx26^{+/-} mice. Both Pax2-Cx26^{+/-} and WT mice were exposed to 96 dB SPL of white noise for 2 hours, one time. The noise-exposed day is defined as day 0. ABR thresholds were normalized to the pre-noise exposure levels. (A and B) Changes of ABR thresholds in Cx26^{+/-} and WT mice after noise exposure. Vertical arrows indicate the noise exposure day. ABRs in (A) and (B) were evoked by 16 and 40 kHz of tone bursts, respectively. In comparison with WT mice, ABR thresholds in Cx26^{+/-} mice were not completely recovered after noise exposure; the ABR thresholds in Cx26^{+/-} mice have ~10 dB SPL of permanent threshold shift. (C) Changes of ABR thresholds in frequency range in Cx26^{+/-} and WT at P1. In comparison with WT mice, Cx26^{+/-} mice have a large ABR threshold increase in a high-frequency range. (D) ABR threshold shift in Cx26^{+/-} mice at P90. In comparison with control Cx26^{+/-} mice without noise exposure; noise-exposed Cx26^{+/-} mice at 3 months after noise exposure have ~10 dB SPL of increase in ABR thresholds in all tested frequency ranges. *P < 0.05 and **P < 0.01, two-tailed t test.

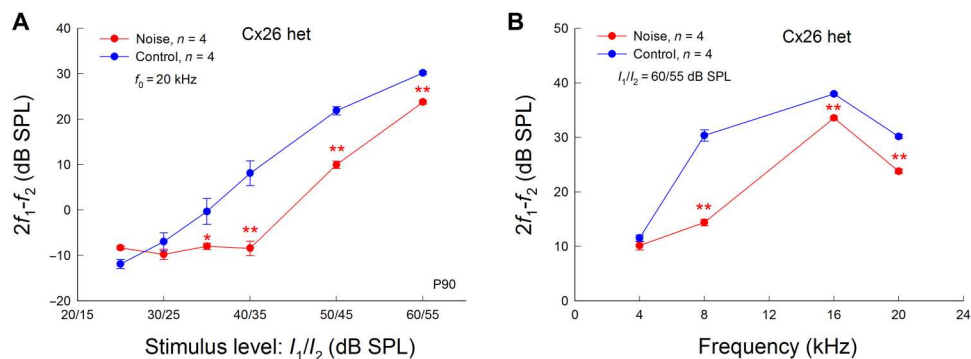


Fig. 9. Reduction of DPOAE in Cx26^{+/-} mice after noise exposure. Mice were 6 months old and 3 months after noise exposure. Cx26^{+/-} mice without noise exposure served as control. (A) Reduction in DPOAE in Cx26^{+/-} mice after noise exposure in the I/O plot. In comparison with control Cx26^{+/-} mice without noise exposure, DPOAE in noise-exposed Cx26^{+/-} mice was significantly reduced. (B) The reduction of DPOAE in the noise-exposed Cx26^{+/-} mice in the frequency range. I₁/I₂ = 60/55 dB SPL. DPOAE in the noise-exposed Cx26^{+/-} mice appears to have significant reduction in comparison with control Cx26^{+/-} mice without noise exposure. *P < 0.05 and **P < 0.01, two-tailed t test.

increased (Fig. 10, B to D). In comparison with the normal control group, DPOAEs in *GJB2* heterozygote carriers were significantly increased by 4 to 8 dB SPL at 2- to 8-kHz frequency range (Fig. 10B). ABR in *GJB2* heterozygote carriers also appeared large (Fig. 10C). In comparison with the normal control group, peaks I, III, VI, and V of ABRs evoked by 25 dB of normal hearing level (nHL) clicks in *GJB2* heterozygote carriers were larger than normal children.

Quantitative analyses (Fig. 10D) showed that the peaks I, II, III, VI, and V of ABRs in *GJB2* heterozygote carriers were 0.070 ± 0.020, 0.011 ± 0.010, 0.092 ± 0.018, 0.144 ± 0.026, and 0.172 ± 0.017 μV, respectively. In comparison with peaks I, II, III, VI, and V (0.026 ± 0.004, 0.001 ± 0.002, 0.074 ± 0.005, 0.095 ± 0.010, and 0.119 ± 0.011 μV, respectively) in the normal control group, peaks I, VI, and V in *GJB2* heterozygote carriers were significantly

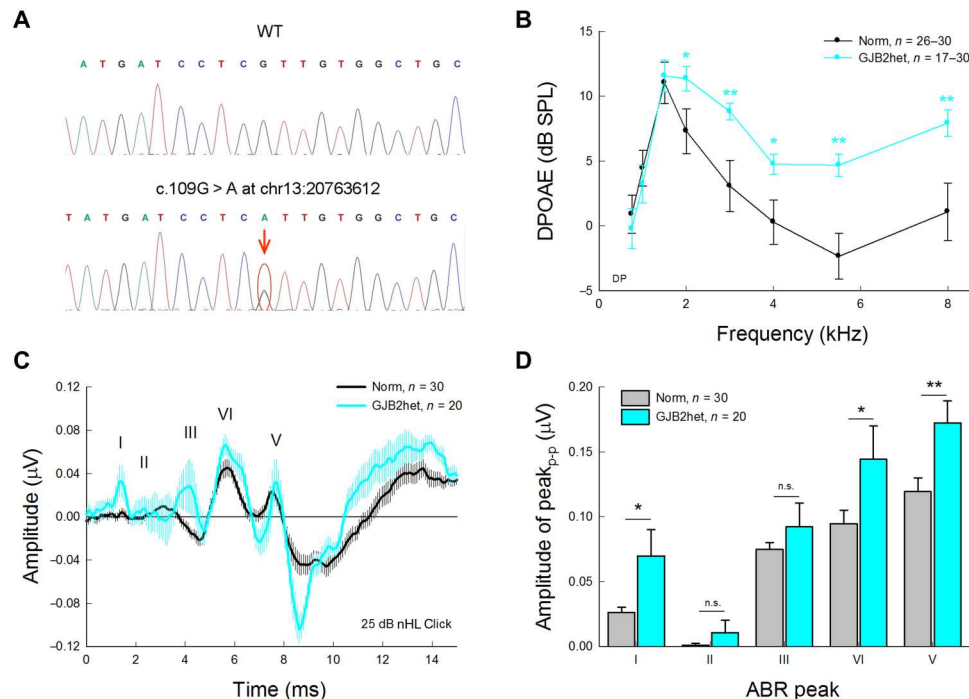


Fig. 10. Human *GJB2* heterozygote carriers have hearing sensitivity, and active cochlear amplification increased. (A) *GJB2* sequence from a heterozygote carrier shows a heterozygous c.109G > A mutant at the antisense strand. Top: *GJB2* sequence from a normal subject. (B) Increased DPOAE in *GJB2* heterozygote carriers. Normal hearing developmental children without mutations served as control. The DPOAE was recorded at $I_1/I_2 = 65/55$ dB SPL. * $P < 0.05$ and ** $P < 0.01$, two-tailed t test. (C) *GJB2* heterozygote carriers have large ABR waves. ABR was evoked by 25 dB of nHL. The traces of ABR recorded from different individuals were averaged. Error bars represent SEM. Apparent increases are visible at ABR peaks I, III, VI, and V recorded from *GJB2* heterozygote carriers. (D) Quantitative measurements of ABR increase in *GJB2* heterozygote carriers. The amplitude (peak-to-peak value) of each peak in individual recordings was measured and averaged. The ABR peaks I, VI, and V recorded from *GJB2* heterozygote carriers were significantly increased in comparison with the normal control group. * $P < 0.05$ and ** $P < 0.01$, one-way ANOVA with a Bonferroni correction. n.s., not significant.

increased ($P = 0.008, 0.048, \text{ and } 0.008$, respectively, one-way ANOVA with a Bonferroni correction) (Fig. 10D).

DISCUSSION

In this study, we found that different from deafness induced by Cx26 homozygous mutation and KO, Cx26 heterozygous mutations or hetero-deletion paradoxically increased hearing sensitivity and active cochlear amplification (Figs. 1, 2, 4, 5, and 10). ABR and CM in both Pax2-Cx26^{+/-} and Foxg1-Cx26^{+/-} hetero-deletion mice were significantly increased (Figs. 1 to 3). DPOAEs in both Pax2-Cx26^{+/-} mice and Foxg1-Cx26^{+/-} mice were also significantly increased, and prestin expression was up-regulated (Figs. 4 and 5). However, EP in Cx26^{+/-} mice was reduced and only had a half of normal value (Fig. 6). Moreover, Prox1-Cx26^{+/-} mice, which only hetero-deleted Cx26 expression in the cochlear supporting cells but not Cx26 deletion in the cochlear lateral wall, had no EP reduction and no ABR and DPOAE increase (Fig. 7). In addition, we further found that Cx26^{+/-} mice were sensitive to noise (Figs. 8 and 9); exposure of the middle level of noise could cause Cx26^{+/-} mice permanent threshold shift (PTS), leading to hearing loss (Fig. 8). Last, as observed in Cx26^{+/-} mice, human Cx26 heterozygous mutation carriers had ABR and DPOAE increased as well (Fig. 10). These data reveal that the Cx26 heterozygous mutations have pathological

changes and can increase hearing sensitivity and susceptibility to noise, leading to hearing loss.

This finding is critically important in the prevention of hearing loss, considering the huge population of *GJB2* heterozygote carriers. As mentioned above, Cx26 heterozygote carriers occupy 10 to 20% of the general population (3, 5, 6). These recessive Cx26 heterozygous mutation carriers have no deafness and have been long considered to be normal in hearing in the clinics. In this study, we found that both Cx26 heterozygous mutation carriers and Cx26^{+/-} hetero-deletion mice had hearing sensitivity and active cochlear amplification increased (Figs. 1 to 5 and 10), indicating that Cx26 heterozygote carriers have hyperacusis-like hearing oversensitivity. Cx26^{+/-} hetero-deletion mice also demonstrated EP reduction (Fig. 6) and were sensitive to noise (Figs. 8 and 9), further indicating that Cx26 heterozygote carriers are vulnerable to noise.

Hyperacusis is a hearing disorder with hearing oversensitivity. Now, the mechanism of hyperacusis remains largely unclear. In particular, little is known about its genetic cues. In this study, we found that Cx26 heterozygous deletion or mutations increased hearing sensitivity by increasing active cochlear amplification (Figs. 1 to 5 and 10) through the up-regulation of prestin expression (Fig. 4, E and F). These data provide a mechanism for hyperacusis and also important information for its genetic cues.

CM in Cx26^{+/-} mice was increased (Fig. 3). However, EP in Cx26^{+/-} mice was reduced (Fig. 6). EP is a driving force for

generation of auditory receptor currents, i.e., CM. Reduction of EP could reduce the driving force to produce auditory receptor currents and decline hearing. It seems contradictory for the observed CM increase in Cx26^{+/-} mice (Fig. 3). However, we previously reported that the hearing function declining can up-regulate prestin expression compensatively to increase active cochlear amplification (30), which can amplify the basilar membrane vibration, leading to increasing auditory receptor currents and hearing sensitivity. Cx26 heterozygous mutation or hetero-deletion to increase hearing sensitivity (i.e., ABR and CM increasing) may share the same mechanism. We found that prestin expression in Cx26^{+/-} mice was up-regulated (Fig. 4, E and F), and DPOAEs in both Cx26 heterozygote carriers and Cx26^{+/-} hetero-deletion mice were increased (Figs. 4, 5, and 10). These data indicate that active cochlear amplification in Cx26^{+/-} mice and heterozygous mutation carriers were enhanced, which could functionally compensate EP reduction and increase the auditory receptor currents (CM) and eventually hearing sensitivity.

This concept is further supported by evidence from Prox1-Cx26^{+/-} heterozygous mice that had no EP reduction and had no hearing sensitivity increased (Fig. 7). Different from whole deletion of Cx26 expression in the cochlea in Pax2-Cx26^{-/-} and Foxg1-Cx26^{-/-} cKO mice (Figs. 1 and 2), Cx26 expression in the cochlear lateral wall in Prox1-Cx26^{-/-} cKO mice remained (Fig. 7, A to C) (16, 17). EP in Prox1-Cx26^{+/-} hetero-deletion mice also remained normal (Fig. 7D). However, ABR and DPOAE in Prox1-Cx26^{+/-} mice were reduced (Fig. 7, E and F) rather than increased as observed in Pax2-Cx26^{+/-} and Foxg1-Cx26^{+/-} mice (Figs. 1, 2, 4, and 5). Moreover, there are neither prestin up-regulation nor OHC electromotility increase in Prox1-Cx26^{-/-} cKO mice (16). These data in versa prove that Cx26 heterozygous mutations or hetero-deletion in Pax2-Cx26^{+/-} and Foxg1-Cx26^{+/-} mice mainly impaired GJ function in the cochlear lateral wall to compromise EP generation, which consequently caused compensative up-regulation of prestin expression to increase active cochlear amplification and eventually hearing sensitivity (Figs. 1 to 5), because prestin expression is functionally dependent (30). The similar compensative up-regulation of prestin expression to increase active cochlear amplification and hearing sensitivity was also found in the long-term administration of salicylate (aspirin), which can inhibit OHC electromotility to reduce active cochlear amplification (30, 31). Now, the detailed cell signaling pathway for prestin functional regulation remains unclear and needs to be investigated in future studies.

As demonstrated in our previous studies (15, 32), heterozygous gap junctional coupling in the cochlear lateral wall has a critical role in EP generation. Cx26 and Cx30 are major isoforms in the cochlea and can form Cx26/Cx30 heterotypic and/or heteromeric GJ channels in the cochlea (12, 21, 33, 34), playing important function in the cochlea and hearing (22, 33). In particular, Cx26/Cx30 heterotypic and/or heteromeric GJ channels in the cochlear lateral wall have a critical role in the EP generation (15, 32). Cx26 hetero-deletion or mutations may impair heterotypic/heteromeric GJ channel function in the cochlear lateral wall, thereby compromising EP generation (15).

Different from increase of hearing sensitivity in Cx26^{+/-} hetero-deletion mice, Cx26^{-/-} cKO mice appeared deaf (Figs. 1G and 2C), even EP in Cx26^{-/-} cKO mice was also significantly reduced (Fig. 6). This is consistent with our previous reports that Cx26 deficiency-induced hearing loss is mainly determined by Cx26 deficiency-induced cochlear developmental disorders rather than EP

reduction (13, 23). In previous studies, we also found that GJs between the cochlear supporting cells can modify OHC electromotility (10, 18). Target deletion of Cx26 expression in the OHC supporting cells (outer pillar cells and Deiters cells) in Prox1-Cx26^{-/-} cKO mice could reduce DPOAEs and increased ABR thresholds (Fig. 7) (16, 17, 18). We demonstrated that reduction of DPOAE in Prox1-Cx26^{-/-} cKO mice mainly results from that the deletion of Cx26 at the OHC supporting cell shifted OHC electromotility and reduced active cochlear amplification, leading to hearing loss (16, 17). These results also demonstrate that Cx26 deficiency has complex effects on hearing function in multiple aspects.

Increment of active cochlear amplification can increase susceptibility to noise. We found that Cx26^{+/-} mice are vulnerable to noise in this study (Figs. 8 and 9). Middle level of noise exposure caused PTS in Cx26^{+/-} mice, leading to hearing loss. This is also consistent with our recent finding that GJs between cochlear supporting cells mediate the efferent control on active cochlear amplification (18). The cochlear efferent system provides negative feedback to the cochlea to control active cochlear amplification and hearing sensitivity to protect hearing from noise. We found that the MOC efferent nerves have innervations with cochlear supporting cells and can uncouple GJs between the cochlear supporting cells (18), which eventually leads to shifting OHC electromotility and reduces active cochlear amplification (10, 18). This also suggests that enhancement of active cochlear amplification in Pax2-Cx26^{+/-} and Foxg1-Cx26^{+/-} hetero-deletion mice (Figs. 4 and 5) and heterozygous mutation carriers (Fig. 10) did not result from the deficiency of the cochlear efferent system. Actually, local deletion of Cx26 expression in the cochlear supporting cells led to reduction of DPOAE (Fig. 7) (16–18). The fact that there is no Cx26 expression in hair cells and neurons (12, 22) further supports this concept.

Last, consistent with animal studies, we found that ABR and DPOAE in *GJB2* heterozygous mutation carriers were significantly increased (Fig. 10). This study reveals that recessive *GJB2* heterozygous mutations, which occupy 10 to 20% in the general population, are not “harmless” for hearing and have a hyperacusis-like hearing oversensitivity disorder. Moreover, this study has an important implication that *GJB2* heterozygous mutation carriers are vulnerable to noise and should avoid noise exposure in daily life.

MATERIALS AND METHODS

Generation of Cx26 deletion mice

Cx26 deletion was generated by a Cre-FloxP technique. Pax2-Cre male mice (the Mutation Mouse Regional Center, Chapel Hill, NC), Foxg1-Cre mice, and Prox1-CreER^{T2} mice (stock numbers 004337 and 022075, respectively, The Jackson Laboratory) were crossed with Cx26^{loxP/loxP} mice (EM00245, European Mouse Mutant Archive) to create Pax2-Cx26, Foxg1-Cx26, and Prox1-Cx26 heterozygous mice (F1 mice). Then, we used heterozygous × heterozygous breeding strategy to generate homozygous [Cre⁺/Cx26^{loxP(+/-)}], heterozygous [Cre⁺/Cx26^{loxP(+/-)}], and WT [Cre⁺/Cx26^{loxP(-/-)} or Cre⁻/Cx26^{loxP(+/-)}] mice (16, 23). For Prox1-Cx26 mice, tamoxifen (T5648, Sigma-Aldrich, St. Louis, MO) was administered to all litters at postnatal day 0 by hypodermic injection (0.5 mg/10 g, ×3 days) (16). WT littermates were used as controls. All experimental procedures were conducted in accordance with the policies of the University of Kentucky Animal Care and Use Committee.

ABR, CM, and DPOAE recordings

ABR, CM, and DPOAE were recorded by use of a Tucker-Davis ABR workstation (Tucker-Davis Tech., Alachua, FL) (16, 23). Mice were anesthetized by intraperitoneal injection with 0.1 ml/10 g (mouse weight) of a mixture of ketamine and xylazine (8.5 ml of saline + 1 ml of ketamine + 0.55 ml of xylazine). Body temperature was maintained at 37° to 38°C. ABR was evoked by both clicks and series of tone bursts (4 to 40 kHz, 10 to 80 dB SPL, a 5-dB step) with an ES-1 high-frequency speaker (Tucker-Davis Tech., Alachua, FL). The signals were amplified by 50,000 and averaged 200 times. The recording filter was set up at 300 to 3000 Hz. The ABR threshold was determined by the lowest level at which an ABR can be recognized. If mice had severe hearing loss, then the ABR test at the intensity range of 70 to 100 dB SPL was used.

CM was evoked by 8-kHz tone bursts and recorded with the same electrode setting as ABR recording as previously reported (16, 23, 35). The signal was amplified by 50,000 with 3- to 50-kHz filter and averaged by 100 times.

For DPOAE recording, two pure tones (f_1 and f_2 ; $f_2/f_1 = 1.22$) were simultaneously delivered into the ear. The test frequencies were presented by a geometric mean of f_1 and f_2 [$f_0 = (f_1 \times f_2)^{1/2}$]. The intensity of f_1 (I_1) was set at 5 dB SPL higher than that of f_2 (I_2). The responses were averaged by 150 times (16, 24).

EP recording

Mice were anaesthetized as described above, and the body temperature was maintained at 37° to 38°C. The trachea was exposed, and the tracheal tube was put into the trachea by cutting along the middle line (13, 24, 32). Then, the cochlea was exposed by a ventral approach, and a small hole was made on the bone over the spiral ligament. A glass pipette filled with a K⁺-based intracellular solution was inserted into the hole (13, 32). The potential was continually recorded as the electrode pipette penetrated through the lateral wall by use of a MultiClamp 700A amplifier (Molecular Devices, CA) and digitized using a Digidata 1322A (Molecular Devices, CA).

Immunofluorescent staining

The cochlear tissue preparation and immunofluorescent staining were performed as we previously described (12, 21). The cochlear cross sections were fixed with 4% paraformaldehyde in 0.1 M phosphate-buffered saline (PBS) (pH 7.4) for 30 min. After washed with 0.1 M PBS for three times, the tissue was incubated in a blocking solution (10% goat serum and 1% bovine serum albumin in the PBS) with 0.1% Triton X-100 for 30 min at room temperature. The tissue then was incubated with primary antibody in the blocking solution at 4°C overnight. Monoclonal mouse anti-Cx26 (1:200 to 1:500; catalog no. 33-5800), polyclonal rabbit anti-Cx30 (1:200 to 1:500; catalog no. 71-2200, Invitrogen Corp., Carlsbad, CA), or polyclonal goat anti-prestin (1:50; catalog no. sc-22694, Santa Cruz Biotechnology Inc., CA) was used. After completely washing out the primary antibodies with PBS, the reaction to a 1:600 dilution of secondary Alexa Fluor 488- or Alexa Fluor 568-conjugated antibodies (Molecular Probes) in the blocking solution followed at room temperature for 1 hour. After completely washing out, the section was mounted with a fluorescence mounting medium (H-1000, Vector Lab, CA) and observed under a Nikon A1R confocal microscope system (36).

For quantitative measure of Cx26, Cx30, and prestin expression, the labeled pixels and intensity in the OC and the cochlear lateral wall were measured by use of ImageJ software [National Institutes of Health (NIH), Bethesda, USA] (15, 37). For prestin labeling, the labeling intensity in OHC area was measured as our previously described (37). The average of labeling intensity was calculated after subtraction of background intensity, and the averaged labeling intensities were normalized to those in WT mice.

Noise exposure

Mice were awake and exposed to white noise (96 dB SPL) for 2 hours, one time, in a small cage under loud speakers in a sound-proof chamber (18, 36). Sound pressure level and spectrum in the cage were measured before experiments.

Participant recruiting

Children in this study were recruited from daily clinical visiting in Shenzhen Maternity and Child Healthcare Hospital, Shenzhen, China, who were previously diagnosed with *GJB2* heterozygous mutations by standard genetic diagnosis, which includes sequencing 24 common deafness genes, such as *GJB2*, *GJB3*, *SCL26A4*, *MYO15A*, *TECTA*, *OTOF*, *MT-RNR1*, and so on. In some cases, full exome sequencing was further performed. Any double or multiple point mutations in *GJB2*, digenic *GJB2* mutations with other common deafness gene mutations, and homozygous *GJB2* mutations were excluded. The control group recruited from normally delivered, typical development, and age-matched children passed from newborn hearing screening tests. The other exclusion criteria in both *GJB2* heterozygote group and normal control groups include the following: active ear pathology such as otitis media with effusion, the presence of other deafness risk factors or deafness gene mutations in a family history, neurological and congenital infections, chromosomal abnormalities, neurocutaneous syndromes, endocrine and metabolic disorders, cleft palate or facial malformations, a history of prematurity, neurodegenerative disease, and severe hypoxic-ischemic encephalopathy. The informed consent was obtained from all the recruited participant's parents or guardians. This project and the data used in this project were approved by the Affiliated Shenzhen Maternity and Child Healthcare Hospital Ethics Committee.

ABR and DPOAE recordings in humans

ABR and DPOAE were recorded by Bio-logic Navigator-Pro Evoked Potential System (Natus Medical Inc., Mundelein, IL, USA). Electrodes were placed on the high forehead (Fz), the ipsilateral mastoid, and the low forehead (FpZ) that served as the non-inverting (+), inverting (−), and ground, respectively. Etymotic Research ER-3 insert earphones were used for ABR recording. Alternating click stimuli were presented at 25 dB of nHL with 19.1/s of presenting rate. The recording time window was 21.33 ms. Responses were amplified by 1,000,000 times, filtered using a 100- to 3000-Hz band-pass filter. For DPOAE recording, two pure tones with the ratio of $f_2/f_1 = 1.22$ and $I_1/I_2 = 65/55$ dB of nHL from 500 Hz to 8 kHz of geometric frequency [$f_0 = (f_1 \times f_2)^{1/2}$] were used. The recording with the signal-to-noise ratio (S/N) > 8 was adopted.

Reproducibility, data processing, and statistical analysis

The numbers of recording mice in each experiment were indicated in the related figure. Each experiment was repeated at least three

times. Data were plotted by SigmaPlot. Error bars represent SEM. Data were expressed as means \pm SEM other than indicated in text. Statistical analyses were performed by SPSS v18.0 (SPSS Inc., Chicago, IL). Parametric and nonparametric data comparisons were performed using one-way ANOVA or Student's *t* tests after assessment of normality and variance. The threshold for significance was $P = 0.05$. Bonferroni post hoc test was used in ANOVA.

Supplementary Materials

This PDF file includes:

Fig. S1

Table S1

REFERENCES AND NOTES

- F. J. del Castillo, I. del Castillo, The DFNB1 subtype of autosomal recessive non-syndromic hearing impairment. *Front Biosci. (Landmark Ed)* **16**, 3252–3274 (2011).
- D. K. Chan, K. W. Chang, GJB2-associated hearing loss: Systematic review of worldwide prevalence, genotype, and auditory phenotype. *Laryngoscope* **124**, E34–E53 (2014).
- P. Dai, F. Yu, B. Han, Y. Yuan, Q. Li, G. Wang, X. Liu, J. He, D. Huang, D. Kang, X. Zhang, H. Yuan, E. Schmitt, D. Han, L.-J. Wong, The prevalence of the 235delC GJB2 mutation in a Chinese deaf population. *Genet. Med.* **9**, 283–289 (2007).
- G. E. Green, D. A. Scott, J. McDonald, G. G. Woodworth, V. C. Sheffield, R. J. Smith, Carrier rates in the midwestern United States for GJB2 mutations causing inherited deafness. *JAMA* **281**, 2211–2216 (1999).
- S.-H. Han, H.-J. Park, E.-J. Kang, J.-S. Ryu, A. Lee, Y.-H. Yang, K.-R. Lee, Carrier frequency of GJB2 (connexin-26) mutations causing inherited deafness in the Korean population. *J. Hum. Genet.* **53**, 1022–1028 (2008).
- D. Wattanasirichaigoon, C. Limwongse, C. Jariengprasert, P. T. Yenchtsomanus, C. Tocharoenthanaphol, W. Thongnoppakhun, C. Thawil, D. Charoenpipop, T. Pho-iam, S. Thongpradit, P. Duggal, High prevalence of V37I genetic variant in the connexin-26 (GJB2) gene among non-syndromic hearing-impaired and control Thai individuals. *Clin. Genet.* **66**, 452–460 (2004).
- L. Zelante, P. Gasparini, X. Estivill, S. Melchionda, L. D'Agurra, N. Govea, M. Milá, M. D. Monica, J. Lutfi, M. Shohat, E. Mansfield, K. Delgrosso, E. Rappaport, S. Surrey, P. Fortina, Connexin26 mutations associated with the most common form of non-syndromic neurosensory autosomal recessive deafness (DFNB1) in Mediterraneans. *Hum. Mol. Genet.* **6**, 1605–1609 (1997).
- H.-B. Zhao, T. Kikuchi, A. Ngezahayo, T. W. White, Gap junctions and cochlear homeostasis. *J. Membr. Biol.* **209**, 177–186 (2006).
- T. Kikuchi, R. S. Kimura, D. L. Paul, J. C. Adams, Gap junctions in the rat cochlea: Immunohistochemical and ultrastructural analysis. *Anat. Embryol. (Berl)* **191**, 101–118 (1995).
- N. Yu, H. B. Zhao, Modulation of outer hair cell electromotility by cochlear supporting cells and gap junctions. *PLOS ONE* **4**, e7923 (2009).
- H. B. Zhao, J. Santos-Sacchi, Auditory collusion and a coupled couple of outer hair cells. *Nature* **399**, 359–362 (1999).
- H.-B. Zhao, N. Yu, Distinct and gradient distributions of connexin26 and connexin30 in the cochlear sensory epithelium of guinea pigs. *J. Comp. Neurol.* **499**, 506–518 (2006).
- J. Chen, J. Chen, Y. Zhu, C. Liang, H.-B. Zhao, Deafness induced by Connexin 26 (GJB2) deficiency is not determined by endocochlear potential (EP) reduction but is associated with cochlear developmental disorders. *Biochem. Biophys. Res. Commun.* **448**, 28–32 (2014).
- Y. Zhu, L. Zong, L. Mei, H.-B. Zhao, Connexin26 gap junction mediates miRNA intercellular genetic communication in the cochlea and is required for inner ear development. *Sci. Rep.* **5**, 15647 (2015).
- L. Mei, J. Chen, L. Zong, Y. Zhu, C. Liang, R. O. Jones, H.-B. Zhao, A deafness mechanism of digenic Cx26 (GJB2) and Cx30 (GJB6) mutations: Reduction of endocochlear potential by impairment of heterogeneous gap junctional function in the cochlear lateral wall. *Neurobiol. Dis.* **108**, 195–203 (2017).
- Y. Zhu, C. Liang, J. Chen, L. Zong, G. D. Chen, H.-B. Zhao, Active cochlear amplification is dependent on supporting cell gap junctions. *Nat. Commun.* **4**, 1786 (2013).
- L. Zong, J. Chen, Y. Zhu, H. B. Zhao, Progressive age-dependence and frequency difference in the effect of gap junctions on active cochlear amplification and hearing. *Biochem. Biophys. Res. Commun.* **489**, 223–227 (2017).
- H.-B. Zhao, L. M. Liu, N. Yu, Y. Zhu, L. Mei, J. Chen, C. Liang, Efferent neurons control hearing sensitivity and protect hearing from noise through the regulation of gap junctions between cochlear supporting cells. *J. Neurophysiol.* **127**, 313–327 (2022).
- A. Forge, D. Becker, S. Casalotti, J. Edwards, N. Marziano, G. Nevill, Gap junctions in the inner ear: Comparison of distribution patterns in different vertebrates and assessment of connexin composition in mammals. *J. Comp. Neurol.* **467**, 207–231 (2003).
- J. Lautermann, W. J. ten Cate, P. Altenhoff, R. Grümmer, O. Traub, H. G. Frank, K. Jahnke, E. Winterhager, Expression of the gap-junction connexins 26 and 30 in the rat cochlea. *Cell Tissue Res.* **294**, 415–420 (1998).
- Y. P. Liu, H. B. Zhao, Cellular characterization of Connexin26 and Connexin30 expression in the cochlear lateral wall. *Cell Tissue Res.* **333**, 395–403 (2008).
- J. C. Wingard, H.-B. Zhao, Cellular and deafness mechanisms underlying connexin mutation-induced hearing loss—A common hereditary deafness. *Front. Cell. Neurosci.* **9**, 202 (2015).
- C. Liang, Y. Zhu, L. Zong, G.-J. Lu, H. B. Zhao, Cell degeneration is not a primary causer for Connexin26 (GJB2) deficiency associated hearing loss. *Neurosci. Lett.* **528**, 36–41 (2012).
- Y. Zhu, J. Chen, C. Liang, L. Zong, J. Chen, R. O. Jones, H.-B. Zhao, Connexin26 (GJB2) deficiency reduces active cochlear amplification leading to late-onset hearing loss. *Neuroscience* **284**, 719–729 (2015).
- F. J. del Castillo, M. Rodríguez-Ballesteros, A. Alvarez, T. Hutchin, E. Leonardi, C. A. de Oliveira, H. Azaiez, Z. Brownstein, M. R. Avenarius, S. Marlin, A. Pandya, H. Shahin, K. R. Siemering, D. Weil, W. Wuyts, L. A. Aguirre, Y. Martin, M. A. Moreno-Pelayo, M. Villamar, K. B. Avraham, H.-H. M. Dahl, M. Kanaan, W. E. Nance, C. Petit, R. J. H. Smith, G. Van Camp, E. L. Sartorato, A. Murgia, F. Moreno, I. del Castillo, A novel deletion involving the connexin-30 gene, del(GJB6-d13s1854), found in trans with mutations in the GJB2 gene (connexin-26) in subjects with DFNB1 non-syndromic hearing impairment. *J. Med. Genet.* **42**, 588–594 (2005).
- D. K. Chan, I. Schrijver, K. W. Chang, Connexin-26-associated deafness: Phenotypic variability and progression of hearing loss. *Genet. Med.* **12**, 174–181 (2010).
- I. Lerer, M. Sagi, Z. Ben-Neriah, T. Wang, H. Levi, D. Abeliovich, A deletion mutation in GJB6 cooperating with a GJB2 mutation in trans in non-syndromic deafness: A novel founder mutation in Ashkenazi Jews. *Hum. Mutat.* **18**, 460 (2001).
- V. Michel, J. P. Hardelin, C. Petit, Molecular mechanism of a frequent genetic form of deafness. *N. Engl. J. Med.* **349**, 716–717 (2003).
- H.-B. Zhao, Hypothesis of K⁺-recycling defect is not a primary deafness mechanism for Cx26 (GJB2) deficiency. *Front. Mol. Neurosci.* **10**, 162 (2017).
- N. Yu, M.-L. Zhu, B. Johnson, Y. P. Liu, R. O. Jones, H.-B. Zhao, Prestin up-regulation in chronic salicylate (aspirin) administration: An implication of functional dependence of prestin expression. *Cell. Mol. Life Sci.* **65**, 2407–2418 (2008).
- Z. W. Huang, Y. Luo, Z. Wu, Z. Tao, R. O. Jones, H.-B. Zhao, Paradoxical enhancement of active cochlear mechanics in long-term administration of salicylate. *J. Neurophysiol.* **93**, 2053–2061 (2005).
- J. Chen, Y. Zhu, C. Liang, J. Chen, H. B. Zhao, Pannexin1 channels dominate ATP release in the cochlea ensuring endocochlear potential and auditory receptor potential generation and hearing. *Sci. Rep.* **5**, 10762 (2015).
- H.-B. Zhao, Directional rectification of gap junctional voltage gating between dieters cells in the inner ear of guinea pig. *Neurosci. Lett.* **296**, 105–108 (2000).
- H.-B. Zhao, J. Santos-Sacchi, Voltage gating of gap junctions in cochlear supporting cells: Evidence for nonhomotypic channels. *J. Membr. Biol.* **175**, 17–24 (2000).
- J. Chen, C. Liang, L. Zong, Y. Zhu, H. B. Zhao, Knockout of pannexin-1 induces hearing loss. *Int. J. Mol. Sci.* **19**, 1332 (2018).
- H.-B. Zhao, Y. Zhu, L.-M. Liu, Excess extracellular K⁺ causes inner hair cell ribbon synapse degeneration. *Commun. Biol.* **4**, 24 (2021).
- N. Yu, M.-L. Zhu, H.-B. Zhao, Prestin is expressed on the whole outer hair cell basolateral surface. *Brain Res.* **1095**, 51–58 (2006).

Acknowledgments

Funding: This work was supported by NIH grants R01 DC017025 and R01 DC019687 to H.-B.Z. and the National Natural Science Foundation of China (grant number: 82000974) to C.L. **Author contributions:** H.-B.Z. designed experiments. L.-M.L., S.F., J.C., C.L., and H.-B.Z. performed experiments. L.-M.L., C.L., S.F., J.C., and H.-B.Z. analyzed data. H.-B.Z. wrote the paper. L.-M.L., C.L., S.F., and J.C. reviewed the paper. **Competing interests:** The authors declare that they have no competing interests. **Data and materials availability:** All data needed to evaluate the conclusions in the paper are present in the paper and/or the Supplementary Materials.

Submitted 19 October 2022

Accepted 10 January 2023

Published 8 February 2023

10.1126/sciadv.adf4144